Journal of Ecology and Environment

RESEARCH Open Access

Quantifying how urban landscape heterogeneity affects land surface temperature at multiple scales

Ehsan Rahimi[1*], Shahindokht Barghjelveh[1] and Pinliang Dong[2]

Abstract

Background: Landscape metrics have been widely applied to quantifying the relationship between land surface temperature and urban spatial patterns and have received acceptable verification from landscape ecologists but some studies have shown their inaccurate results. The objective of the study is to compare landscape metrics and texture-based measures as alternative indices in measuring urban heterogeneity effects on LST at multiple scales.

Results: The statistical results showed that the correlation between urban landscape heterogeneity and LST increased as the spatial extent (scale) of under-study landscapes increased. Overall, landscape metrics showed that the less fragmented, the more complex, larger, and the higher number of patches, the lower LST. The most significant relationship was seen between edge density (ED) and LST ($r = -0.47$) at the sub-region scale. Texture measures showed a stronger relationship (R^2 = 34.84% on average) with LST than landscape metrics (R^2 = 15.33% on average) at all spatial scales, meaning that these measures had a greater ability to describe landscape heterogeneity than the landscape metrics.

Conclusion: This study suggests alternative measures for overcoming landscape metrics shortcomings in estimating the effects of landscape heterogeneity on LST variations and gives land managers and urban planners new insights into urban design.

Keywords: Land surface temperature, Landscape heterogeneity, Texture-based measures, Landscape metrics

Introduction

Land surface temperature (LST) of cities is warmer than suburbs due to impervious surfaces and buildings (Li et al. 2012; Tuttle et al. 2006). This phenomenon is due to the change of natural habitats into cities, parking lots, roads, and other impervious surfaces that considerably affect the local weather. A combination of natural and anthropogenic covers in cities results in high heterogeneity. This heterogeneity affects the ecological processes and biodiversity of urban areas, which ultimately change the urban ecosystems functioning (Cushman and Huettmann, 2010). Numerous studies have estimated the relationship between LST and urban landscape heterogeneity, especially green spaces (Asgarian et al. 2015; Chen et al. 2014; Connors et al. 2013; Li et al. 2012; Sahana et al., 2016; Zhang et al. 2009; Zhang et al., 2013; Zheng et al. 2014). Nowadays, it is well-known that increasing the area of green spaces reduces LST values (Essa et al. 2013; Mallick et al. 2013; Yue et al. 2007; Zheng et al. 2014), but there are conflicting results about how the spatial arrangement of these green spaces affect LST. Some studies have claimed that higher fragmentation of green spaces positively affects LST (Bao et al. 2016; Li et al. 2011; Maimaitiyiming et al. 2014), whereas other studies have shown a negative effect (Kong et al. 2014; Masoudi and Tan, 2019; Masoudi et al. 2019; Xie et al. 2013).

Estimating the relationship between LST and green spaces patterns is an essential step for lowering LST in a city because it is possible to reduce the city's temperature by creating new green space patches. Therefore, there is an urgent need for quantifying the effects of urban landscape heterogeneity on LST correctly (Cadenasso et al. 2007). It is acknowledged that

* Correspondence: ehsanrahimi666@gmail.com
[1]Environmental Sciences Research Institute, Shahid Beheshti University, Tehran, Iran
Full list of author information is available at the end of the article

the relationship between landscape patterns and LST is scale-dependent (Ma et al. 2016; Zhou et al. 2017). Therefore performing multi-scale analysis is necessary to understand the relationship between urban patterns and LST (Li et al. 2018; Lu et al. 2020). Most studies have examined the relationship between landscape patterns and LST at a single scale and less attention has been paid to the hierarchical structure and multi-scales of the relationship (Wu et al. 2019). However, some studies have examined the relationship between urban patterns and LST at different scales. For example, at temporal scales (different seasons), Ma et al. (2016) showed that LST had a positive correlation with the impervious surface in summer daytime/nighttime and winter nighttime, but a negative correlation in winter daytime. At the spatial scales, the relationship between LST and urban heterogeneity has been measured at different pixel sizes (Lu et al. 2020; Xiao et al. 2007) and spatial extents (Myint et al. 2010).

Landscape metrics (McGarigal et al. 2002) and land use maps have frequently been used to investigate the relationship between urban heterogeneity and LST variations in the last years. This kind of discrete model has shown a sufficient capability to measure landscape structure patterns in many studies (Li et al. 2011; Liu and Weng, 2008). However, it has been shown that some metrics, although differently calculated, are highly correlated (Frazier and Kedron, 2017; Kedron et al. 2018; Neel et al. 2004; Turner et al. 2001). Other studies have shown that it is difficult to compare the metrics on different scales (Wu et al. 2002). Therefore, depending on the scale of the study, different results are obtained in landscape ecology (Bolliger et al. 2007). The behavior of the landscape metrics to the spatial and temporal resolution of the existing data has also become an important issue in landscape ecology studies in recent decades (Saura and Castro, 2007; Šímová and Gdulová, 2012). Due to the complexity of the landscape metrics, the choice of appropriate metrics that reflects the characteristics of the landscape has become a challenge (Liu et al. 2013).

As mentioned above, the accuracy of landscape metrics is considerably related to the accuracy of classified maps. The classification of urban areas that are a mixture of different covers is more complicated than other land covers. Therefore, we need new methods to examine urban heterogeneity correctly. One of the suggested alternative methods that can display and analyze urban heterogeneity based on continuous data (e.g., NDVI) are texture-based measures that directly use remote sensing data as their inputs to capture landscape heterogeneity. These measures quantify spatial aspects of landscapes based on the gray-level co-occurrence matrix (GLCM) (Haralick and Shanmugam, 1973). Each GLCM index can highlight a particular property of texture, such as smoothness or coarseness produced by the uniformity or variability of image color or tone (Li and Narayanan, 2004; Park and Guldmann, 2020). Texture analysis methods have been used in the different remote sensing-based analyses, such as analysis of urban growth (Gluch, 2002), forest cover classification (Coburn and Roberts, 2004), habitat selection (Tuttle et al., 2006), and as a predictor of spices richness (Hofmann et al., 2017; Tuanmu and Jetz, 2015). Recent studies have paid attention to these indices and acknowledged their efficiency in measuring landscape heterogeneity. For example, Park and Guldmann (2020) compared the GLCM indices' ability as continuous metrics and landscape metrics as discrete metrics in estimating spatial patterns of tree canopy at the landscape level. They showed that there was a strong relationship between landscape characteristics resulted from GLCM indices and discrete models (landscape metrics).

As far as we are aware, no study has applied GLCM indices in estimating the LST relationship with urban landscape heterogeneity at multiple scales. Given the above background, this study aims to compare landscape metrics and alternative measures (i.e., texture-based measures) in determining the effects of urban heterogeneity on LST. In the present study, we first retrieve land surface temperature and land cover maps of Tehran City in the year 2017 using Landsat images. Next, we estimate the effects of urban composition and configuration on LST values using landscape metrics and texture-based measures at multiple scales and compare the ability of these metrics in quantifying the relationship between LST and urban structure elements like buildings and green spaces.

Methods

Study area

Tehran has experienced the fastest population growth among the other cities in Iran, Tehran, with an area of 750 km^2, is a metropolis of 10 million inhabitants and locating on the southern side of the Alborz (a mountain range in northern Iran) (Sodoudi et al., 2014) (Fig. 1). This city divides into 22 areas and each area has its municipal administration that tries to provide adequate services to citizens. These 22 areas are different in size, amount of green spaces, paved surface, and buildings; hence, there are significant variations in LST temperatures. The annual mean temperature changes between 15 °C and 18 °C, and given the parts of different heights, there is a 3 °C difference in other districts' temperatures.

Spatial data

We used Landsat image in the year 2017 as initial data for deriving LST and land cover maps. Landsat 8 TIRS sensor has two TIR bands (band 10 and 11), a spatial resolution of 30 m, and a 12-bit radiometric resolution. To compare landscape metrics and texture measures in measuring LST changes, we applied the maximum

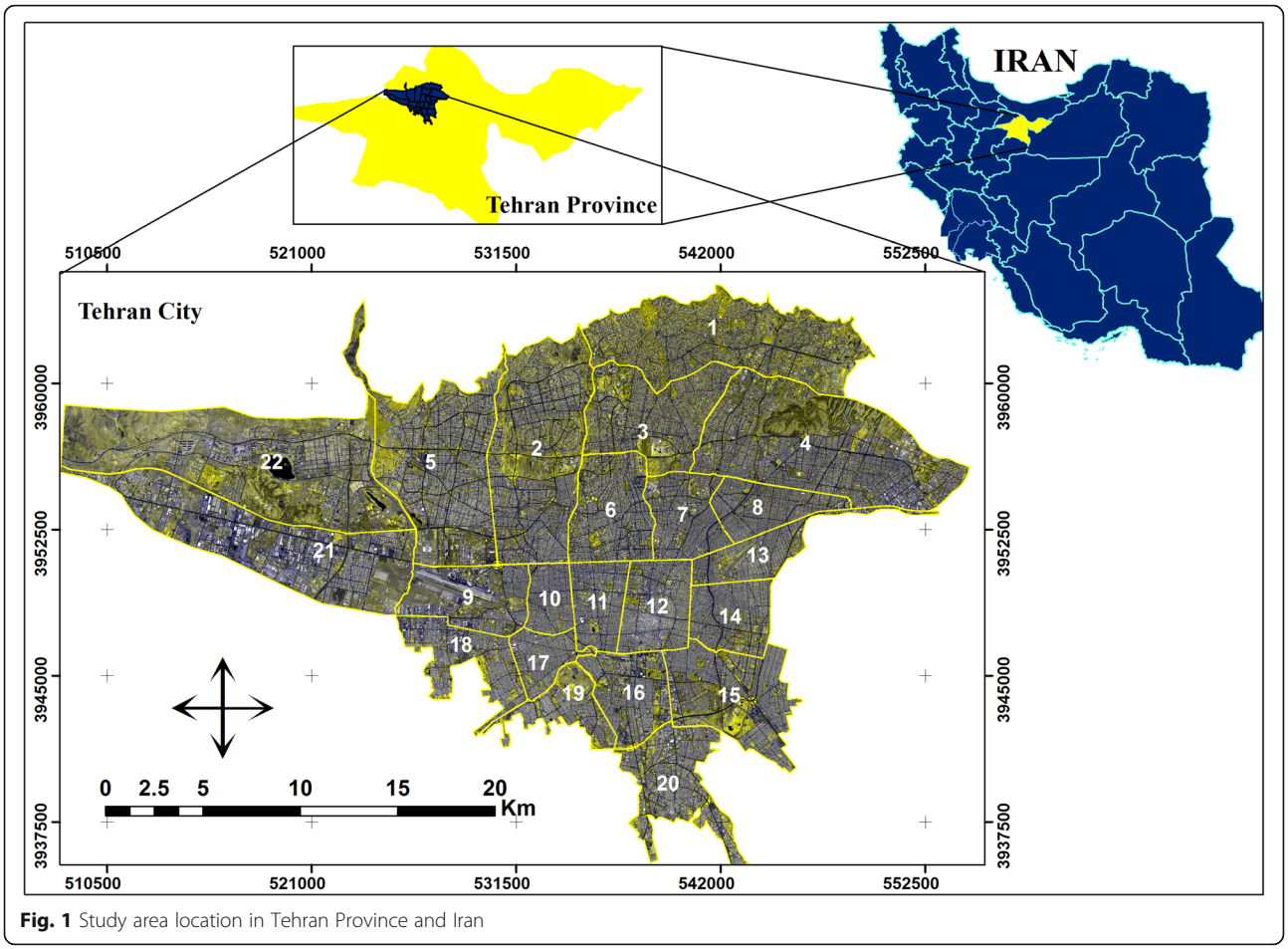

Fig. 1 Study area location in Tehran Province and Iran

likelihood algorithm to classify Landsat image as the input image for calculating landscape metrics. The study area was classified into five classes, including green spaces (trees, parks, and natural vegetation covers), built-up areas, impervious surfaces (roads, parking areas, and cement surfaces), bare soils (useless lands without vegetation cover), and water (artificial lakes). The image was acquired during the growing season and is freely available at the Landsat archive at the United States Geological Survey (USGS) (http://glovis.usgs.gov).

Calculation of LST

We used the split-window method for Landsat 8 TIRS (Sahana et al. 2016) to retrieve Tehran LST maps (Eq. 1).

$$\begin{aligned} \mathrm{LST} = {} & TB_{10} + C_1(TB_{10} - TB_{11}) \\ & + C_2(TB_{10} - TB_{11})^2 + C_0 + (C_3 + C_4 W) \\ & \times (1-\varepsilon) + (C_5 + C_6 W)\triangle\varepsilon \end{aligned} \quad (1)$$

Elements of LST equations and their explanations are presented in Table 1, split window constant-coefficient values are included in Table 2, and thermal constant values for TIR bands are presented in Table 3.

Based on the equation below, we converted TB_{10} and TB_{11} to top atmospheric spectral radiance (Eq. 2);

$$\mathrm{TOA} = M_L \times \mathrm{DN} + A_L \quad (2)$$

The brightness temperature (T_B) for TB_{10} and TB_{11}bands calculated based on the following formula (Eq. 3);

$$T_B = \frac{K_2}{\ln\left(\frac{K_1}{TOA} + 1\right)} \quad (3)$$

Landscape metrics

In this study, we applied landscape metrics to compare texture-based indices in estimating the relationship between urban landscape patterns and LST. For this purpose, eight landscape metrics including, number of patches (NP), patch density (PD), percentage of landscape (PLAND), edge density (ED), total edge (TE), perimeter-area fractal dimension (PAFRAC), splitting index (SPLIT), and landscape shape index (Ferreira et al., 2020.) were

Table 1 Elements of LST equations and their explanations

Elements	Explanation
TB	Surface temperature
LST	Land surface temperature
TB_{10}	The brightness temperature of band 10
TB_{11}	The brightness temperature of band 11
ε	Mean band 10 and band 11
W	The atmospheric water vapor content
$\Delta\varepsilon$	Difference in LSE
DN	Digital number
TB	The brightness temperature for both 10 and 11
TOA	Atmospheric spectral radiance

calculated using Fragstats software (McGarigal et al. 2002) at class and landscape levels (Table 4).

Note a_{ij} = area (m^2) of patch, A = total landscape area (m^2), n_i = number of class i patches in the landscape, e_{ij} = total length (m) of edges of patch ij, including landscape boundary, c = area (m^2) within patch ij separated from its boundary by a user-specified buffer width (m), g_{ii} = the number of adjacencies (contiguity) between pixels of patch class i, $max\ g_{ii}$ = maximum possible number of adjacencies among pixels of patches of class i, h_{ij} = distance (m) from patch ij to the nearest neighboring patch of the same type (class), based on patch edge-to-edge distance, computed from cell center to cell center (McGarigal et al. 2002)

Vegetation indices

In the continuous framework, we need to use continuous indices that reflect landscape patterns for measuring landscape fragmentation. In this regard, we used the normalized difference vegetation index (NDVI) as an alternative indicator of landscape patterns. The normalized difference vegetation index is useful for identifying green vegetation biomass (Fan and Myint, 2014), and is the most widely used index for many different applications, ranging from vegetation monitoring to urban sprawl (Nolè et al. 2014). The equation for calculating the NDVI index is as follows (Eq. 4).

Table 2 Split window constant-coefficient values

Constant	Value
C0	− 0.268
C1	1.378
C2	0.183
C3	54.3
C4	− 2.238
C5	− 129.2
C6	16.4

Table 3 Thermal constant values for TIR bands

Constant	Band 10	Band 11
K_1	774.89	480.89
K_2	1321.08	1201.14
Radiance multiplier (M_L)	0.0003342	0.0003342
Radiance add (A_L)	0.1	0.1

$$\mathrm{NDVI} = \frac{R_{\mathrm{NIR}} - R_{RED}}{R_{\mathrm{NIR}} + R_{RED}} \tag{4}$$

Where Red and NIR stand for the spectral reflectance measurements acquired in the red (visible. and near-infrared regions, respectively.

Texture-based measures

We applied two types of texture measures to the NDVI index as input images: first- and second-order measures (Table 5). The first-order measures describe the frequency distribution of pixels without regarding the pixel of neighbors. The second-order measures are based on the probability of observing a pair of values at two pixels within a specific distance (Tuanmu and Jetz, 2015). We used eight texture measures including, variance, mean, contrast, dissimilarity, entropy, homogeneity, correlation, and energy (Table 5) for quantifying urban landscape heterogeneity.

Determining the relationship between LST and urban green space

The relationship between spatial patterns of green space in Tehran and surface temperature was determined at multi-scales. To determine the relationship between LST and landscape metrics, first, 100 random points were created throughout Tehran City, and then the landscape around each of these points was determined with a radius of 1 km. In the next step, the relationship between the spatial patterns of the green space of these 100 landscapes with their mean LST was investigated. Also, the relationship between green spaces and LST was determined at the scale of 22 districts (sub-region) of Tehran. The relationship between LST and texture measures was examined at three scales of pixels (pixel-based), the radius of 1 km around the random points, and 22 districts of Tehran.

We used Pearson correlation, linear regression, and stepwise multiple regression analysis to estimate the relationship between LST maps and spatial patterns of green spaces. We use the stepwise method, which starts at the forward selection, but at each stage, the possibility of deleting a predictor, as backward elimination, is

Table 4 Descriptions of the selected landscape metrics.

Category	Metric	Equation	Range
Area and Edge			
	PLAND	$C_1(TB_{10} - TB_{11})$	0 ≤ PLAND ≤ 100
	TE	$\sum e_{ik}$	TE ≥ 0, without limit.
	ED	$\frac{\sum e_{ik}}{A}(10000)$	0 ≤ ED, no limit
Shape	PAFRAC	$\frac{[(\sum \ln p_{ij} - \ln a_{ij})] - [(\sum \ln p_{ij})(\sum \ln a_{ij})]^2}{(\sum \ln p_{ij}^2) - (\sum \ln p_{ij})}$	1 ≤ PAFRAC ≤ 2
Aggregation	LSI	$\frac{0.25\sum e_{ik}}{\sqrt{A}}$	1 ≤ LSI, no limit
	SPLIT	$\frac{A^2}{\sum A_{ij}^2}$	1 ≤ SPLIT ≤ number of cells in the landscape area squared
	NP	n_i	NP ≥ 1, without limit
	PD	$\frac{n_i}{A}(10000)(100)$	PD > 0, constrained by cell size

considered (Chong and Jun, 2005). The probability value to enter variables into the stepwise models was set at 0.05 and the probability to remove was set at 0.1. The selection of measures in the multiple stepwise regression test was based on the variance inflation factor (VIF), so that we removed measures with VIF > 10 from the analysis to prevent multicollinearity.

Results

Land use map and spatial heterogeneity of green spaces

Figure 2 shows the land cover map of Tehran City classified into five classes acquired from Landsat 8 data in the year 2017. According to Fig. 2, most of the green spaces patches are located in the north and the west of Tehran and less amount of this class is in the center and the south. Therefore, based on visual interpretation, there is an aggregated pattern of vegetation covers, mostly concentrated in the north of Tehran City. Figure 3 shows the spatial heterogeneity of green spaces in the 22 municipal districts based on landscape metrics. In this figure, for each district, the spatial patterns of green spaces are measured using landscape metrics, and the arrangement of green space patches in the city of Tehran is shown based on the areas under municipal management.

For example, the SPLIT metric (Fig. 3A) measures the aggregation degree of patches. SPLIT equals 1 when the landscape consists of a single patch and increases as the focal patch type is increasingly reduced in area and subdivided into smaller patches. According to this index, most municipal districts of Tehran have an aggregated arrangement of green space patches. The PD metric shows the patch density of green spaces. The maximum PD is gained when every cell is a separate patch. This metric (Fig. 3B) shows that two districts in the northern parts of Tehran have the highest density of patches and the western and central areas have the lowest density. The LSI metric (Fig. 3C) measures the irregularities in the shape of patches and increases as landscape shape becomes more irregular. This index shows that in the

Table 5 Texture metrics as measures of spatial landscape heterogeneity

Metric	Value range	Expected relationship[a]	Equation
First-order texture			
Variance	≥ 0	*H*~*X*	$\sum_i^{N_g}\sum_j^{N_g}(i-\mu)^2 p(i,j)$
Mean	≥ 0	*H*~*X*	$\sum_k^{N_g} k p_{x-y}(k)$
Second-order texture			
Contrast	≥ 0	*H*~*X*	$\sum_i^{N_g}\sum_j^{N_g}(i-j)^2 p_d(i,j)$
Dissimilarity	≥ 0	*H*~*X*	$\sum_i^{N_g}\sum_j^{N_g} p(i,j)\lvert i-j\rvert$
Entropy	≥ 0	*H*~*X*	$-\sum_i^{N_g}\sum_j^{N_g} p(i,j)\ log[p(i,j)]$
Homogeneity	≥ 0; ≤ 1	*H*~–*X*	$\sum_i^{N_g}\sum_j^{N_g}\frac{1}{1+(i-j)^2} p_d(i,j)$
Correlation	≥ 0; ≤ 0	*H*~–*X*	$\sum_i^{N_g}\sum_j^{N_g} p_d(i,j)\frac{(i-\mu_x)(j-\mu_y)}{\sigma_x\sigma_y}$
Energy	≥ 0; ≤ 1	*H*~–*X*	$\sum_i^{N_g}\sum_j^{N_g} g_{ig^2}$

[a]*H*~*X*, larger values indicate greater heterogeneity; *H* ~ –*X*, lower values indicate greater heterogeneity.

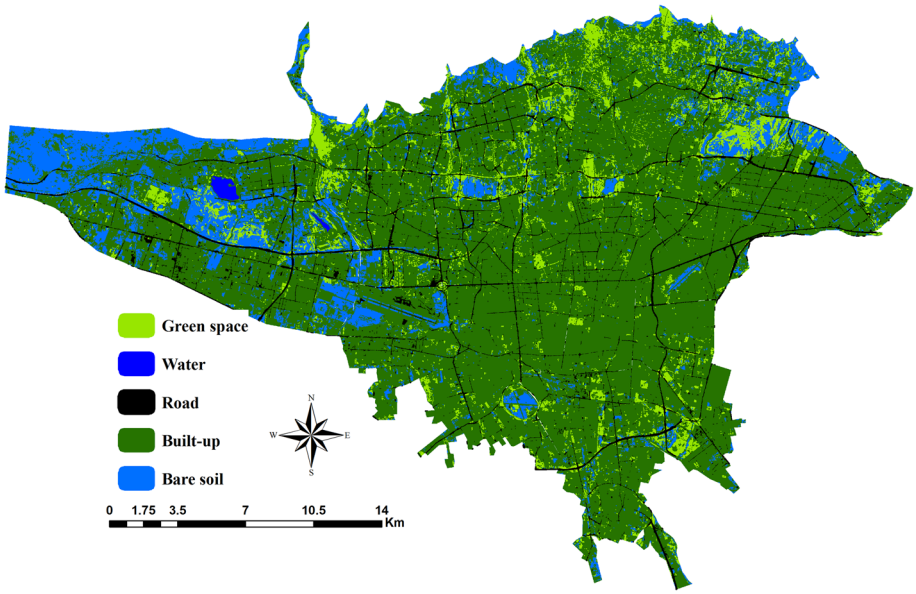

Fig. 2 Land cover map of the study area in 2017

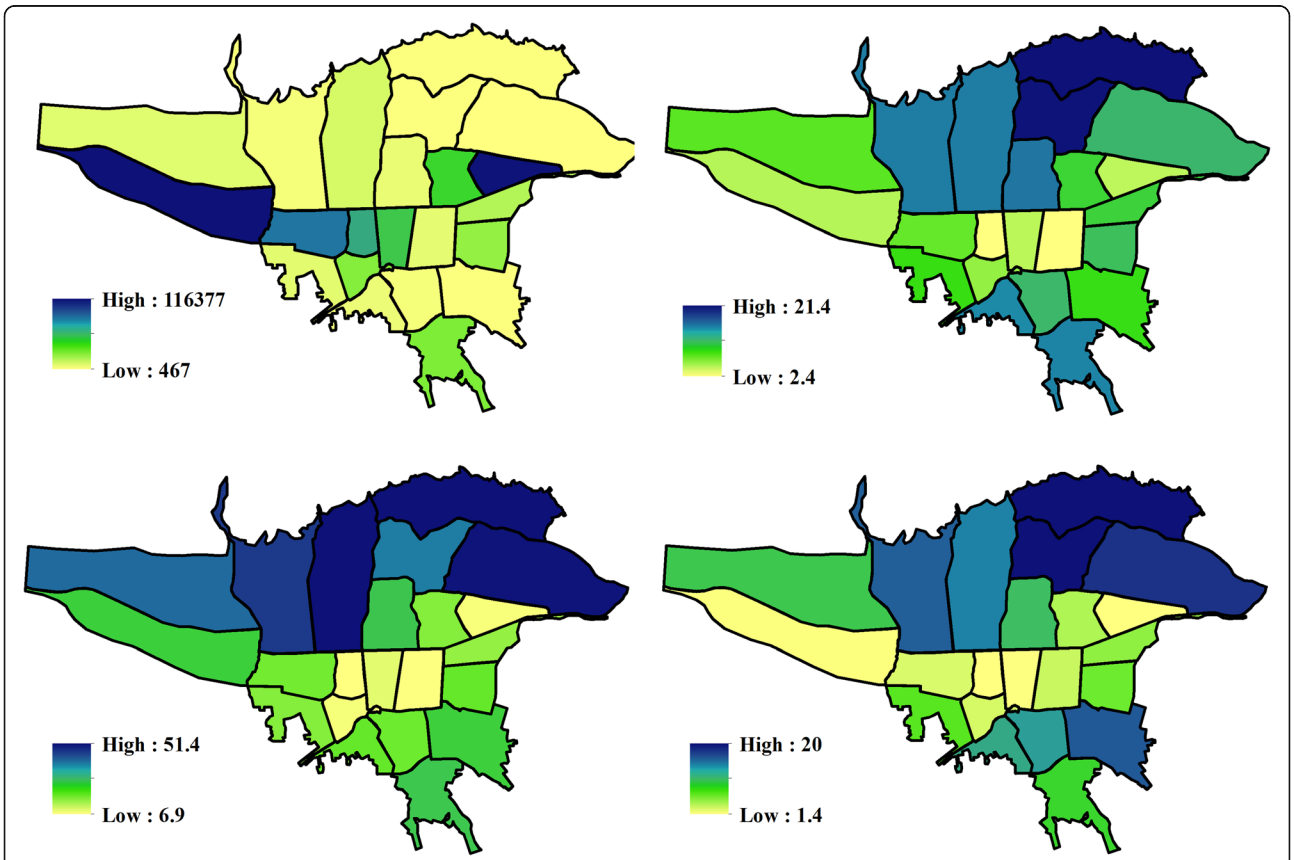

Fig. 3 Spatial heterogeneity of green spaces in the 22 municipal districts based on landscape metrics. (**A**) SPLIT, (**B**) PD, (**C**) LSI, and (**D**) PLAND

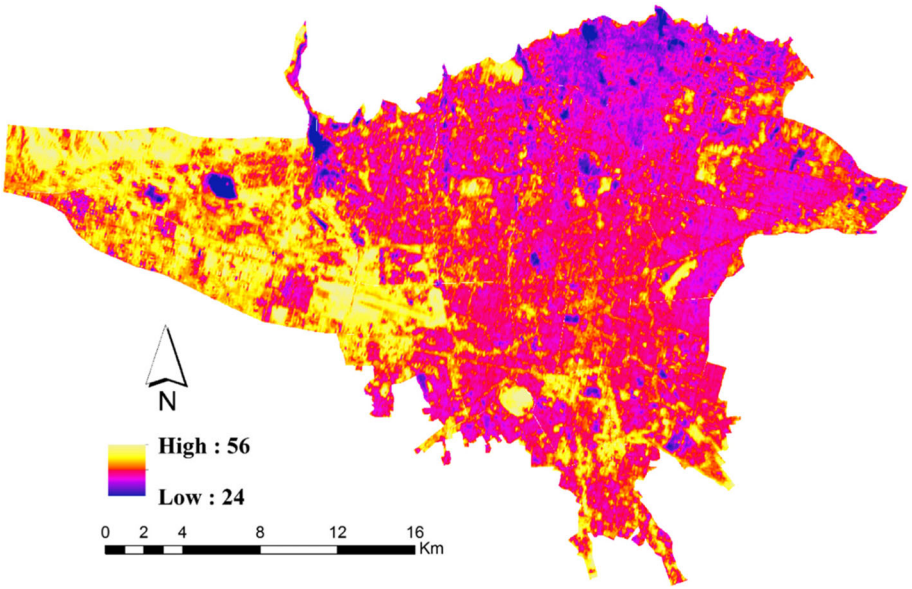

Fig. 4 LST map of Tehran city in the year 2017

northern parts of Tehran, green spaces are irregular and more complex.

Estimating the relationship between landscape metrics and LST

Figure 4 shows the land surface temperature map of Tehran city in the year 2017. The LST map shows that the northern areas of Tehran, which have more green spaces than other areas, have lower temperatures. The western regions of the city, which include barren lands, show the highest surface temperatures. Table 6 shows the results of the regression analysis and the Pearson correlation coefficient between the landscape metrics and the LST map at two scales. At the sub-region scale, the LST has the highest correlation with the patch density (PD) and edge density of green patches ($r = -0.47$), and approximately 22% of the changes in surface temperature in Tehran are explained by these metrics (R^2 = 22.3% and 22.7% respectively). The lowest correlation is also seen between the LSI metric and LST ($r = -0.24$). The linear relationships between landscape metrics and LST are not statistically significant, as the values of R^2 vary from 5.9 to 22.7% (15.33% averaged). The last row (at sub-region scale) shows the result of multiple stepwise regression tests. The result of this test shows that only the ED metric has been selected as the best subset of the landscape metrics, which explains 22.7% of the changes in LST. At the 1000 m scale, the statistical relationships between landscape metrics and LST are weaker than the sub-region scale. The highest correlation is seen between LST and the three metrics LSI, NP, and PD ($r = -34$). LST also has the lowest correlation with the PAFRAC metric ($r = -0.03$). The results of linear regression also do not show a strong statistical relationship between LST and landscape metrics, and on average these metrics explain only 7.5% of LST changes within a radius of 1 km from random points. Stepwise regression has also chosen the PD metric as the most effective metric that can only explain 7.11% of the LST changes.

Table 6 Linear and multiple stepwise regression functions and Pearson correlation (*r*) coefficients between landscape metrics of green space and LST

Scale	Equation	*r*	R^2	*P* value
Sub-region	LST = 41.44–0.14 PLAND	− 0.42	17.9%	0.05
	LST = 40.70–0.001 NP	− 0.30	9.3%	0.16
	LST = 42.30–0.16 PD	− 0.47	22.3%	0.02
	LST = 41.77–0.02 ED	− 0.47	22.7%	0.02
	LST = 57.24–12.10 PAFRAC	− 0.16	14.6%	0.07
	LST = 40.62–0.02 TE	− 0.33	11.1%	0.01
	LST = 41.13–0.03 LSI	− 0.24	5.9%	0.27
	LST = 39.67 + 0.042 SPLIT	0.33	11.5%	0.12
	LST = 47.127–0.0317 ED	–	22.7%	0.02
1000m	LST = 45.95–0.06084 PLAND	− 0.19	3.6%	0.04
	LST = 46.69–0.03922 NP	− 0.34	12%	0.00
	LST = 46.72–0.1246 PD	− 0.34	12.1%	0.00
	LST = 46.23–0.000050 TE	− 0.26	7.2%	0.00
	LST= 46.25–0.01583 ED	− 0.27	7.3%	0.00
	LST = 47.43–0.2533 LSI	− 0.34	11.9%	0.00
	LST= 46.21–0.678 PAFRAC	− 0.03	0.1%	0.70
	LST = 45.46 + 0.000000 SPLIT	0.24	6.1%	0.00
	LST = 46.227–0.0901 PD	–	7.11%	0.08

Estimating the relationship between texture measures and LST

Figure 5 shows the texture metrics applied to the NDVI index. The dissimilarity measure (Fig. 5A) indicates more dissimilarity around green patches. The energy measure shows the highest energy in barren lands (Fig. 5B), while these areas have the highest entropy (Fig. 5C). The homogeneity measure shows the highest heterogeneity in the northern regions of Tehran (Fig. 5B). According to this classification, the interpretation of their results is similar for each group of measures. Table 7 presents the results of the statistical relationship between LST and texture-based measures at three scales. According to this table, some measures have a high correlation with LST, and others have a weak correlation. For example at the sub-region scale, the highest positive correlation is seen between energy measure and LST (r = 0.72). However, the lowest correlation is observed between variance measure and LST (r = 0.02), which is not statistically significant. Contrast and correlation measures also have a weak correlation with LST (r = − 0.17 and 0.25, respectively). The linear relationship between texture measures and LST also showed that the energy measure has the strongest correlation with the LST as this measure could explain 52% of the LST changes in Tehran City. On average, texture measures explained 34.84% of LST changes at the sub-region scale. The last row (at sub-region scale) shows the result of the multiple stepwise regression test. According to this test, correlation, energy, and mean measures have been selected as the best subset of texture measures to explain changes in LST, which can predict 86.08% of its changes.

At the 1000 m scale, the statistical relationships between texture measures and LST are weaker than the sub-region scale. At this scale, LST has the highest correlation with the entropy (r = − 0.54) and the lowest correlation with the contrast (r = − 0.008). The results of linear regression also show that texture measures can explain an average of 14.96% of LST changes. However, multiple regression shows (the last row at 1000 m scale) that the measures of correlation, dissimilarity, entropy, and mean can explain 62.6% of LST changes. At the pixel-based scale, the relationship between LST and texture measures is not as high as the previous scales. At this scale, LST has the highest correlation with the mean measure (r = − 0.29) and the results of linear regression show that on average these measures can explain 2.4% of LST changes. According to the results of stepwise regression (the last row), the four measures of variance,

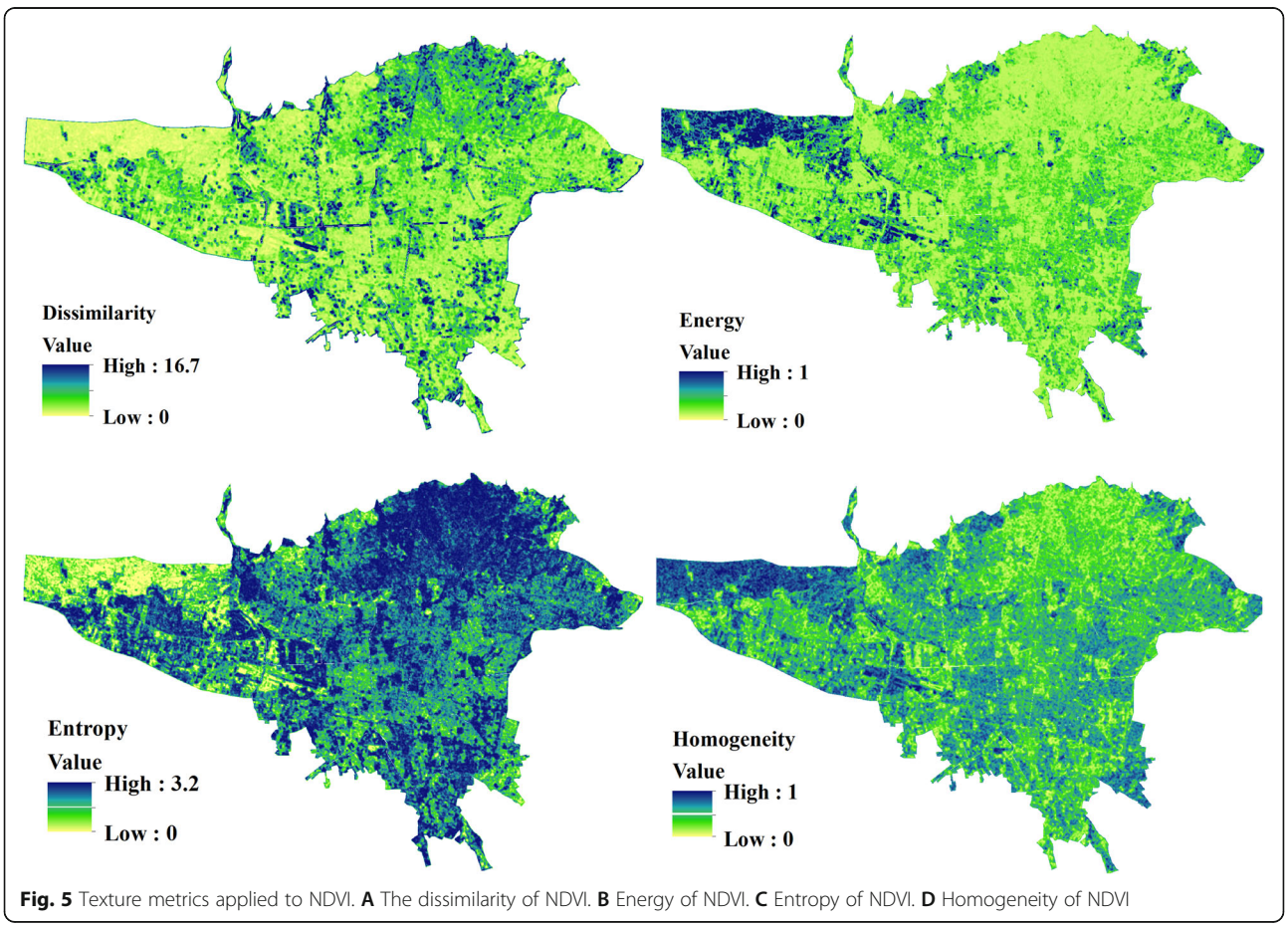

Fig. 5 Texture metrics applied to NDVI. **A** The dissimilarity of NDVI. **B** Energy of NDVI. **C** Entropy of NDVI. **D** Homogeneity of NDVI

Table 7 The Linear and multiple stepwise regression statistics and Pearson correlation coefficient of texture measures with LST in 2017

Scale	Equation	*r*	R^2	*P* value
Sub-region	LST = 43.01 − 0.04 contrast of NDVI	− 0.17	3.2%	0.4
	LST = 44.75 − 0.04 mean of NDVI	− 0.67	44.9%	0.01
	LST = 30.89 + 0.08 energy of NDVI	0.72	52.1%	0.00
	LST = 50.45 − 0.04 entropy of NDVI	− 0.70	49.5%	0.00
	LST = 42.37 − 0.03 variance of NDVI	− 0.02	0%	0.99
	LST = 35.70 + 0.04 homogeneity of NDVI	0.69	48.1%	0.01
	LST = 32.19 + 0.04 correlation of NDVI	0.25	6.6%	0.23
	LST = 44.02 − 0.04 dissimilarity of NDVI	− 0.48	23.1%	0.02
	LST = 14.331 + 3.530 correlation + 4.02 energy − 0.1744 mean	–	86.08%	0.00
1000m	LST = 45.95 − 0.02556 contrast of NDVI	− 0.08	0.7%	0.40
	LST = 52.60 − 0.4834 mean of NDVI	− 0.51	26.9%	0.00
	LST = 43.75 + 15.00 energy of NDVI	0.45	20.7%	0.00
	LST= 55.21 − 3.831 entropy of NDVI	− 0.54	29.4%	0.00
	LST = 45.74 − 0.01540 variance of NDVI	0.03	0.2%	0.68
	LST = 39.67 + 12.55 homogeneity of NDVI	0.53	28.3%	0.00
	LST = 44.40 + 4.502 correlation of NDVI	0.17	3.1%	0.00
	LST = 48.08 − 1.151 dissimilarity of NDVI	− 0.35	10.4%	0.00
	LST = 59.69 + 10.91 correlation + 1.481 dissimilarity − 3.940 entropy − 0.7064 mean	–	62.6%	0.00
Pixel-based	LST = 45.74 + 0.000720 contrast of NDVI	0.006	0.00	0.83
	LST = 48.94 − 0.2259 mean of NDVI	− 0.29	9%	0.00
	LST = 44.79 + 8.686 energy of NDVI	0.19	3.8%	0.00
	LST = 48.91 − 1.256 entropy of NDVI	− 0.18	3.3.%	0.00
	LST = 45.72 + 0.001848 variance of NDVI	0.01	0%	0.68
	LST = 44.11 + 3.437 homogeneity of NDVI	0.18	3.3%	0.00
	LST = 45.57 + 0.7066 correlation of NDVI	− 0.06	0.4%	0.10
	LST = 46.05 − 0.1361 dissimilarity of NDVI	− 0.07	0.6%	0.10
	LST = 43.90 + 0.04853 variance − 0.4057 mean + 2.113 entropy + 15.16 energy	–	17.3%	0.00

mean, entropy, and energy can explain 17.3% of the LST changes.

Discussion

Effects of landscape composition and configuration on LST

On the whole, there was a weak relationship between landscape metrics and LST in the present study, so that ED metrics could explain 22.7% of LST changes at the sub-region scale. However, by the reduction of the scale of analysis to the landscapes with a radius of 1 km, this relationship became weaker (R = 7.3%) and was not satisfactory. This result suggests that larger scales are more suitable for examining the relationship between metrics and LST because at smaller scales there is less green space in the landscape that cannot reduce the LST well (Myint et al. 2010). In addition, tiny green patches are usually merged into large patches in classified maps of satellite images, and the elimination of these patches on a small scale may be effective.

At the sub-region scale, our results that showed increasing the area of green spaces resulted in decreasing LST is consistent with other studies (Guo et al. 2019; Li et al. 2012). Two metrics including the percentage of landscape (PLAND), and the number of patches (NP) of green space class were negatively correlated (r = − 0.42 and − 0.30, respectively) with LST. Chen et al. (2014) found that PLAND explained about 56% of the mean LST. Still, in the current study, PLAND demonstrated 17.9% of LST variations, implying that the configurational aspects of landscape structure were more capable to measure LST variations than compositional structure. Masoudi and Tan (2019) and Masoudi et al. (2019) found that area-related metrics (PLAND, LPI, and MPS) were negatively correlated with LST for different

understudy cities. Guo et al. (2019) observed a negative correlation of mean patch size (MPS) and the largest patch index (LPI) with LST that confirmed our results.

The most significant correlation was between edge density (ED) and patch density (PD) of patches and LST (r = − 0.47), suggesting fragmented and shape-complicated green space patches reduce LST. In several studies, higher LST has been associated with higher PD of green spaces, which is concluded to be a more fragmented pattern (Fan et al. 2015; Li et al. 2012; Zhang et al. 2009; Zhou et al. 2011). However, McGarigal et al. (2002) frankly acknowledge that patch density (PD) has limited interpretive value by itself because it conveys no information about the sizes and configuration of patches, and selecting the neighbor rule for calculating PD affects the results. Jaeger (2000) also discussed the limitations of this metric for evaluating habitat fragmentation and concluded that PD behavior changes during the fragmentation process. Interpreting results based on the PD metric does not always lead to an accurate conclusion. Masoudi and Tan (2019) and Masoudi et al. (2019) showed that PD was positively and AI negatively correlated with LST for all study areas and concluded that less fragmentation (lower PD) and higher aggregation resulted in cooling effects of urban green spaces.

Positive impacts of aggregation have been reported in several studies (Estoque et al. 2017; Li et al. 2012; Xie et al. 2013; Zhang et al. 2009; Zheng et al. 2014; Zhibin et al. 2015), whereas Li et al. (2012), Maimaitiyiming et al. (2014) and Bao et al. (2016) showed negative impacts. For the built-up class, a more fragmented and edge-complicated pattern of unvegetated surfaces has been shown to have a warmer LST than vegetated surfaces (Zhou et al. 2011). Zhou et al. (2011) found a negative correlation between LST and patch density of paved surfaces and a positive correlation between LST and patch density of buildings. They suggested that fragmented built-up class (higher PD) led to higher LST. The earlier studies have concluded their results based on the belief that higher PD means higher fragmentation. Still, our research shows that this statement is not always accurate because the SPLIT (r = 0.33) metric showed that less-fragmented and clustered vegetation cover in Tehran city resulted in lower LST (Table 6). SPLIT metric approaches 1 when the landscape; consists of a single patch and increases as the focal patch type increasingly losses its area and is subdivided into smaller patches (McGarigal et al. 2002). Therefore, relationship between LST and aggregation metrics like SPLIT showed that fragmented green space affects LST adversely.

All shape complexity metrics (ED, TE, LSI, and PAFRAC) were negatively correlated with LST, consistent with many studies (Asgarian et al. 2015; Bao et al. 2016; Chen et al. 2014; Estoque et al. 2017; Guo et al. 2019; Li et al. 2012; Zhou et al. 2011), suggesting the positive effects of more complex shapes in reducing LST. Li et al. (2012) concluded that green spaces configuration metrics affected LST significantly, particularly for LSI and ED that were negatively correlated. Guo et al. (2019) also showed a positive effect of edge density (ED) on LST. However, Kong et al. (2014), Masoudi et al. (2019), Xie et al. (2013), and Masoudi and Tan (2019) indicated that shape complexity metrics (ED, LSI), especially ED and LSI of green spaces were positively correlated with LST in all cities under study, implying that the more complex shapes affected LST values negatively.

In the present study, landscape configuration was generally observed to have more significant effects on LST than composition, similar results have been shown with several studies (Chen et al. 2014; Guo et al. 2019; Zhang et al. 2009). Although a weak statistical relationship was observed between landscape metrics and LST, our results showed that less-fragmented (lower SPLIT), more complicated in shape (higher ED and LSI), larger, and the number of patches lead to lower LST. The less-fragmented pattern of green spaces led to a decrease in the land surface temperature, one reason is that with increasing fragmentation, large patches became smaller and the distance between them increases. Reducing the size of the patches causes the green spaces to create less shade and the temperature of the surrounding areas to dominate the temperature inside the patches (Osborne and Alvares-Sanches, 2019). Large patches also have a lower temperature than small patches (especially in the center) and edge effects are more effective on small patches. The complexity of the patches also reduced the LST, one possible reason is that the complicated patches increased edge density might enhance energy flow to surrounding areas, leading to decreased LST (Guo et al. 2019; Wu et al. 2021).

The relationship between texture measures and LST

Statistical analyses showed that the correlation between texture measures and LST increased with increasing scale. This result indicates that the relationship between LST and urban patterns is strongly scale-dependent, but most studies examine this relationship at a single scale. Few studies have investigated the effects of landscape patterns on LST at various scales. For example, Song et al. (2014) found that as the pixel size increases, the correlation between LST and urban patterns increases, and they stated that two resolutions 660 m and 720 m were the best spatial resolutions to measure LST-landscape relationships. Some studies have reported the highest correlations between NDVI and LST in cell sizes 210 to 240 (Lu et al. 2020) and claimed that the changes in the correlation with the changes in cell size indicate the existence of a threshold distance for the cooling

effect of green spaces. Xiao et al. (2007) also found an increase in correlation between built-up density and LST when cell size increased from 30 m to 960 m. Myint et al. (2010) found that the correlation between air temperature and impervious surfaces declined after reaching a window size of 210 m. The reason is that in small scale, green spaces cannot reduce LST considerably and sometimes we consider a small part of a large green space patch in these scales. As the spatial area or window size increases, there will be more green space, and green space patches will be fully considered in the analysis, which can significantly reduce the LST (Myint et al. 2010).

Texture-based measures often have a high correlation with each other and can be divided into two groups based on measuring and displaying landscape heterogeneity: (1) measures that depict greater heterogeneity with higher values (e.g., mean, variance, contrast, dissimilarity, and entropy) and (2) measures that display greater heterogeneity with lower values (e.g., homogeneity, correlation, and energy). Among texture measures used in this study for estimating the relationship between LST and landscape heterogeneity at the sub-region scale, the energy of NDVI showed the strongest correlation with LST (R^2 = 52.1%), which was a second-order texture measure. The higher values of the energy measure show greater heterogeneity (Tuanmu and Jetz, 2015). Therefore, the positive correlation between the energy of NDVI and LST (r = 0.72) implies that LST values increase when vegetation covers are fragmented and dispersed. This result is consistent with landscape metrics, which indicated clustered and homogeneous vegetation covers had lower LST values than dispersed patterns.

In the present study, texture measures showed a stronger relationship (R^2 = 34.84% averaged) with LST than landscape metrics (R^2 = 15.33% averaged) at all scales, meaning that texture measures had a greater ability to show landscape heterogeneity than the landscape metrics examined in the study. Also, a comparison of the results of multiple stepwise regression of landscape metrics and texture measures showed that there was a significant difference between the ability of texture measures to explain changes of LST. Among the landscape metrics, only edge density (ED) was selected as the best predictor of LST changes (R^2 = 22.7%) at the sub-region scale. However, three measures of mean, energy, and correlation were able to predict more than 86% of LST changes. One possible reason is that the accuracy of landscape metrics is strongly dependent on the accuracy of classified maps (Li and Wu, 2004; Shao and Wu, 2008) and the errors related to the land use classification are inevitable and may lead to unreal results (Shao and Wu, 2008). The uncertainties related to the classification process of continuous variables into discrete classes can also reduce the efficiency and accuracy of these metrics (Dormann, 2007; Frazier and Kedron, 2017; Kedron et al., 2018; Park and Guldmann, 2020). Therefore, the uncertainty associated with classification can compromise the reliability of landscape metrics derived from the thematic maps (Cockx et al., 2014; Fan and Myint, 2014; Kedron et al., 2018; Rocchini et al., 2013). Many other factors affect the accuracy and applicability of landscape metrics, like data source accuracy, scale effects, and ecological interpretation (Frazier and Kedron, 2017; Liu et al., 2013). Texture measures have been used in various studies and have shown acceptable ability in ecological studies (Hofmann et al. 2017; St-Louis et al. 2014; Tuanmu and Jetz, 2015; Wood et al. 2013).

Conclusion

In general, our results showed that (1) texture measures can better describe the relationships between LST and green space patterns than landscape metrics, and (2) as the scale increased, the correlation between LST and urban heterogeneity increased. The result was the same for landscape metrics and texture measures. This result indicates that to determine the effects of urban patterns on LST, analyzes should be performed at several scales. Most of the studies that have aimed to estimate the relationship between LST and landscape heterogeneity have applied landscape metrics to achieve this goal. Still, many scientists have criticized these metrics and the accuracy of their results is often controversial.

In this study, some texture measures indicated an acceptable capability to determine the relationship between landscape heterogeneity and land surface temperature. However, others were not suitable for estimating this relationship and showed a weak ability to explain changes in LST, especially at small scales. Therefore, in applying these measures, it is suggested to consider this issue. We also suggest applying these continuous measures instead of using landscape metrics when the spatial arrangement of landscape elements is very heterogeneous. Using these indices saves time and is much more suitable for examining time series analysis than landscape metrics. They provide visual interpretation and can distinguish small changes in the landscape. We performed the statistical analysis at three scales to compare the performance of landscape metrics and texture measures in estimating the effects of green spaces on LST. For each of these scales, the mean values of LST were compared with the mean values of texture measures and landscape metrics. Our suggestion for future studies is to apply more scales with different pixel and extent sizes.

Abbreviations

LST: Land surface temperature; NDVI: Normalized Difference Vegetation Index; NP: Number of patches; MPS: Mean patch size; PD: Patch density; ED: Edge density; TE: Total edge; PLAND: Percentage of landscape; PAFRAC: Perimeter-area fractal dimension; LSI: Landscape Shape Index; SPLIT: Splitting Index; VIF: Variance inflation factor

Acknowledgements

Not applicable

Authors' contributions
ER has written the paper and has done the modeling part of the analysis. ShB has reviewed the paper, helped to write, and helped with the interpretation of the results. PD has reviewed the paper and helped with the interpretation of the results. All authors read and approved the final manuscript.

Funding
There are no financial conflicts of interest to disclose.

Availability of data and materials
Data are available on request from the authors only based on logical requests.

Declarations

Ethics approval and consent to participate
Not applicable

Consent for publication
Not applicable

Competing interests
All authors declare that they have no competing interests.

Author details
[1]Environmental Sciences Research Institute, Shahid Beheshti University, Tehran, Iran. [2]Department of Geography and the Environment, University of North Texas, Denton, USA.

Received: 11 August 2021 Accepted: 19 October 2021
Published online: 13 November 2021

References

Asgarian A, Amiri BJ, Sakieh Y. Assessing the effect of green cover spatial patterns on urban land surface temperature using landscape metrics approach. Urban Ecosyst. 2015;18(1):209–22. https://doi.org/10.1007/s11252-014-0387-7.

Bao T, Li X, Zhang J, Zhang Y, Tian S. Assessing the distribution of urban green spaces and its anisotropic cooling distance on urban heat island pattern in Baotou, China. ISPRS Int J Geo Inf. 2016;5(2):12. https://doi.org/10.3390/ijgi5020012.

Bolliger, J., Wagner, H. H., Turner, M. G., 2007, Identifying and quantifying landscape patterns in space and time, in Kienast, F., Wildi, O. and Ghosh, S., eds., A Changing World: Challenges for Landscape Research, Landscape Series. Berlin: Springer, pp. 177-194. https://link.springer.com/book/10.1007%2F978-1-4020-4436-6.

Cadenasso ML, Pickett ST, Schwarz K. Spatial heterogeneity in urban ecosystems: reconceptualizing land cover and a framework for classification. Front Ecol Environ. 2007;5(2):80–8. https://doi.org/10.1890/1540-9295(2007)5[80:SHIUER]2.0.CO;2.

Chen A, Yao L, Sun R, Chen L. How many metrics are required to identify the effects of the landscape pattern on land surface temperature? Ecol Indic. 2014;45:424–33. https://doi.org/10.1016/j.ecolind.2014.05.002.

Chong I-G, Jun C-H. Performance of some variable selection methods when multicollinearity is present. Chemom Intel Lab Syst. 2005;78(1-2):103–12. https://doi.org/10.1016/j.chemolab.2004.12.011.

Coburn C, Roberts AC. A multiscale texture analysis procedure for improved forest stand classification. Int J Remote Sensing. 2004;25(20):4287–308. https://doi.org/10.1080/0143116042000192367.

Cockx K, Van de Voorde T, Canters F. Quantifying uncertainty in remote sensing-based urban land-use mapping. Int J Appl Earth Observ Geoinform. 2014;31:154–66. https://doi.org/10.1016/j.jag.2014.03.016.

Connors JP, Galletti CS, Chow WT. Landscape configuration and urban heat island effects: assessing the relationship between landscape characteristics and land surface temperature in Phoenix, Arizona. Landsc Ecol. 2013;28(2):271–83. https://doi.org/10.1007/s10980-012-9833-1.

Cushman SA, Huettmann F. Spatial complexity, informatics, and wildlife conservation: Springer; 2010. https://doi.org/10.1007/978-4-431-87771-4.

Dormann CF. Effects of incorporating spatial autocorrelation into the analysis of species distribution data. Glob Ecol Biogeogr. 2007;16(2):129–38. https://doi.org/10.1111/j.1466-8238.2006.00279.x.

Essa W, van der Kwast J, Verbeiren B, Batelaan O. Downscaling of thermal images over urban areas using the land surface temperature–impervious percentage relationship. Int J Appl Earth Observ Geoinform. 2013;23:95–108. https://doi.org/10.1016/j.jag.2012.12.007.

Estoque RC, Murayama Y, Myint SW. Effects of landscape composition and pattern on land surface temperature: An urban heat island study in the megacities of Southeast Asia. Sci Total Environ. 2017;577:349–59. https://doi.org/10.1016/j.scitotenv.2016.10.195.

Fan C, Myint S. A comparison of spatial autocorrelation indices and landscape metrics in measuring urban landscape fragmentation. Landscape Urban Planning. 2014;121:117–28. https://doi.org/10.1016/j.landurbplan.2013.10.002.

Fan C, Myint SW, Zheng B. Measuring the spatial arrangement of urban vegetation and its impacts on seasonal surface temperatures. Prog Phys Geography. 2015;39(2):199–219. https://doi.org/10.1177/0309133314567583.

Ferreira PA, Boscolo D, Lopes LE, Carvalheiro LG, Biesmeijer JC, da Rocha PLB, et al. Forest and connectivity loss simplify tropical pollination networks. Oecologia. 2020;192(2):577–90. https://doi.org/10.1007/s00442-019-04579-7.

Frazier AE, Kedron P. Landscape metrics: past progress and future directions. Curr Landscape Ecol Reports. 2017;2(3):63–72. https://doi.org/10.1007/s40823-017-0026-0.

Gluch R. Urban growth detection using texture analysis on merged Landsat TM and SPOT-P data. Photogram Eng Remote Sensing. 2002;68(12):1283–8.

Guo G, Wu Z, Chen Y. Complex mechanisms linking land surface temperature to greenspace spatial patterns: Evidence from four southeastern Chinese cities. Sci Total Environ. 2019;674:77–87. https://doi.org/10.1016/j.scitotenv.2019.03.402.

Haralick RM, Shanmugam K. Textural features for image classification. IEEE Trans Syst Man Cybern. 1973;6(6):610–21. https://doi.org/10.1109/TSMC.1973.4309314.

Hofmann S, Everaars J, Schweiger O, Frenzel M, Bannehr L, Cord AF. Modelling patterns of pollinator species richness and diversity using satellite image texture. PLoS One. 2017;12(10):e0185591. https://doi.org/10.1371/journal.pone.0185591.

Jaeger JA. Landscape division, splitting index, and effective mesh size: new measures of landscape fragmentation. Landsc Ecol. 2000;15(2):115–30. https://doi.org/10.1023/A:1008129329289.

Kedron PJ, Frazier AE, Ovando-Montejo GA, Wang J. Surface metrics for landscape ecology: A comparison of landscape models across ecoregions and scales. Landsc Ecol. 2018;33(9):1489–504. https://doi.org/10.1007/s10980-018-0685-1.

Kong F, Yin H, James P, Hutyra LR, He HS. Effects of spatial pattern of greenspace on urban cooling in a large metropolitan area of eastern China. Landscape Urban Planning. 2014;128:35–47. https://doi.org/10.1016/j.landurbplan.2014.04.018.

Li C, Zhao J, Thinh NX, Yang W, Li Z. Analysis of the spatiotemporally varying effects of urban spatial patterns on land surface temperatures. Journal of Environ Eng Landscape Manag. 2018;26(3):216–31. https://doi.org/10.3846/jeelm.2018.5378.

Li H, Wu J. Use and misuse of landscape indices. Landsc Ecol. 2004;19(4):389–99. https://doi.org/10.1023/B:LAND.0000030441.15628.d6.

Li J, Narayanan RM. Integrated spectral and spatial information mining in remote sensing imagery. IEEE Trans Geosci Remote Sensing. 2004;42(3):673–85. https://doi.org/10.1109/TGRS.2004.824221.

Li J, Song C, Cao L, Zhu F, Meng X, Wu J. Impacts of landscape structure on surface urban heat islands: A case study of Shanghai, China. Remote Sens Environ. 2011;115(12):3249–63. https://doi.org/10.1016/j.rse.2011.07.008.

Li X, Zhou W, Ouyang Z, Xu W, Zheng H. Spatial pattern of greenspace affects land surface temperature: evidence from the heavily urbanized Beijing metropolitan area, China. Landsc Ecol. 2012;27(6):887–98. https://doi.org/10.1007/s10980-012-9731-6.

Liu D, Hao S, Liu X, Li B, He S, Warrington D. Effects of land use classification on landscape metrics based on remote sensing and GIS. Environ Earth Sci. 2013;68(8):2229–37. https://doi.org/10.1007/s12665-012-1905-7.

Liu H, Weng Q. Seasonal variations in the relationship between landscape pattern and land surface temperature in Indianapolis, USA. Environ Monit Assess. 2008;144(1):199–219. https://doi.org/10.1007/s10661-007-9979-5.

Lu L, Weng Q, Xiao D, Guo H, Li Q, Hui W. Spatiotemporal variation of surface urban heat islands in relation to land cover composition and configuration: a multi-scale case study of Xi'an, China. Remote Sens (Basel). 2020;12(17):2713. https://doi.org/10.3390/rs12172713.

Ma Q, Wu J, He C. A hierarchical analysis of the relationship between urban impervious surfaces and land surface temperatures: spatial scale

dependence, temporal variations, and bioclimatic modulation. Landsc Ecol. 2016;31(5):1139–53. https://doi.org/10.1007/s10980-016-0356-z.
Maimaitiyiming M, Ghulam A, Tiyip T, Pla F, Latorre-Carmona P, Halik Ü, et al. Effects of green space spatial pattern on land surface temperature: Implications for sustainable urban planning and climate change adaptation. ISPRS J Photogram Remote Sensing. 2014;89:59–66. https://doi.org/10.1016/j.isprsjprs.2013.12.010.
Mallick J, Rahman A, Singh CK. Modeling urban heat islands in heterogeneous land surface and its correlation with impervious surface area by using night-time ASTER satellite data in highly urbanizing city, Delhi-India. Adv Space Res. 2013;52(4):639–55. https://doi.org/10.1016/j.asr.2013.04.025.
Masoudi M, Tan PY. Multi-year comparison of the effects of spatial pattern of urban green spaces on urban land surface temperature. Landscape Urban Planning. 2019;184:44–58. https://doi.org/10.1016/j.landurbplan.2018.10.023.
Masoudi M, Tan PY, Liew SC. Multi-city comparison of the relationships between spatial pattern and cooling effect of urban green spaces in four major Asian cities. Ecol Indic. 2019;98:200–13. https://doi.org/10.1016/j.ecolind.2018.09.058.
McGarigal K, Cushman SA, Neel MC, Ene E. FRAGSTATS: spatial pattern analysis program for categorical maps; 2002.
Myint SW, Brazel A, Okin G, Buyantuyev A. Combined effects of impervious surface and vegetation cover on air temperature variations in a rapidly expanding desert city. GIScience Remote Sensing. 2010;47(3):301–20. https://doi.org/10.2747/1548-1603.47.3.301.
Neel MC, McGarigal K, Cushman SA. Behavior of class-level landscape metrics across gradients of class aggregation and area. Landsc Ecol. 2004;19(4):435–55. https://doi.org/10.1023/B:LAND.0000030521.19856.cb.
Nolè G, Lasaponara R, Lanorte A, Murgante B. Quantifying urban sprawl with spatial autocorrelation techniques using multi-temporal satellite data. Int J Agric Environ Inform Sys. 2014;5(2):19–37. https://doi.org/10.4018/IJAEIS.2014040102.
Osborne PE, Alvares-Sanches T. Quantifying how landscape composition and configuration affect urban land surface temperatures using machine learning and neutral landscapes. Comput Environ Urban Systems. 2019;76:80–90. https://doi.org/10.1016/j.compenvurbsys.2019.04.003.
Park Y, Guldmann J-M. Measuring continuous landscape patterns with Gray-Level Co-Occurrence Matrix (GLCM) indices: an alternative to patch metrics? Ecol Indic. 2020;109:105802. https://doi.org/10.1016/j.ecolind.2019.105802.
Rocchini D, Foody GM, Nagendra H, Ricotta C, Anand M, He KS, et al. Uncertainty in ecosystem mapping by remote sensing. Comput Geosci. 2013;50:128–35. https://doi.org/10.1016/j.cageo.2012.05.022.
Sahana M, Ahmed R, Sajjad H. Analyzing land surface temperature distribution in response to land use/land cover change using split window algorithm and spectral radiance model in Sundarban Biosphere Reserve, India. Model Earth Syst Environ. 2016;2(2):81. https://doi.org/10.1007/s40808-016-0135-5.
Saura S, Castro S. Scaling functions for landscape pattern metrics derived from remotely sensed data: Are their subpixel estimates really accurate? ISPRS J Photogram Remote Sensing. 2007;62(3):201–16. https://doi.org/10.1016/j.isprsjprs.2007.03.004.
Shao G, Wu J. On the accuracy of landscape pattern analysis using remote sensing data. Landsc Ecol. 2008;23(5):505–11. https://doi.org/10.1007/s10980-008-9215-x.
Šímová P, Gdulová K. Landscape indices behavior: a review of scale effects. Appl Geography. 2012;34:385–94. https://doi.org/10.1016/j.apgeog.2012.01.003.
Sodoudi S, Shahmohamadi P, Vollack K, Cubasch U, Che-Ani A. Mitigating the urban heat island effect in megacity Tehran. Adv Meteorol. 2014;2014:1–19. https://doi.org/10.1155/2014/547974.
Song J, Du S, Feng X, Guo L. The relationships between landscape compositions and land surface temperature: Quantifying their resolution sensitivity with spatial regression models. Landscape Urban Planning. 2014;123:145–57. https://doi.org/10.1016/j.landurbplan.2013.11.014.
St-Louis V, Pidgeon AM, Kuemmerle T, Sonnenschein R, Radeloff VC, Clayton MK, et al. Modelling avian biodiversity using raw, unclassified satellite imagery. Phil Trans Royal Soc London B Biol Sci. 2014;369(1643):20130197. https://doi.org/10.1098/rstb.2013.0197.
Tuanmu MN, Jetz W. A global, remote sensing-based characterization of terrestrial habitat heterogeneity for biodiversity and ecosystem modelling. Glob Ecol Biogeogr. 2015;24(11):1329–39. https://doi.org/10.1111/geb.12365.
Turner, M. G., Gardner, R. H., O'neill, R. V., 2001, Landscape ecology in theory and practice (Vol.401). New York: Springer.
Tuttle EM, Jensen RR, Formica VA, Gonser RA. Using remote sensing image texture to study habitat use patterns: a case study using the polymorphic white-throated sparrow (Zonotrichia albicollis). Glob Ecol Biogeogr. 2006;15(4):349–57. https://doi.org/10.1111/j.1466-822X.2006.00232.x.
Wood EM, Pidgeon AM, Radeloff VC, Keuler NS. Image texture predicts avian density and species richness. PLoS One. 2013;8(5):e63211. https://doi.org/10.1371/journal.pone.0063211.
Wu C, Li J, Wang C, Song C, Haase D, Breuste J, et al. Estimating the Cooling Effect of Pocket Green Space in High Density Urban Areas in Shanghai, China. Front Environ Sci. 2021;9:181. https://doi.org/10.3389/fenvs.2021.657969.
Wu J, Shen W, Sun W, Tueller PT. Empirical patterns of the effects of changing scale on landscape metrics. Landsc Ecol. 2002;17(8):761–82. https://doi.org/10.1023/A:1022995922992.
Wu Q, Tan J, Guo F, Li H, Chen S. Multi-scale relationship between land surface temperature and landscape pattern based on wavelet coherence: the case of metropolitan Beijing, China. Remote Sens (Basel). 2019;11(24):3021. https://doi.org/10.3390/rs11243021.
Xiao R-B, Ouyang Z-Y, Zheng H, Li W-F, Schienke EW, Wang X-K. Spatial pattern of impervious surfaces and their impacts on land surface temperature in Beijing, China. J Environ Sci. 2007;19(2):250–6. https://doi.org/10.1016/S1001-0742(07)60041-2.
Xie M, Wang Y, Chang Q, Fu M, Ye M. Assessment of landscape patterns affecting land surface temperature in different biophysical gradients in Shenzhen, China. Urban Ecosyst. 2013;16(4):871–86. https://doi.org/10.1007/s11252-013-0325-0.
Yue W, Xu J, Tan W, Xu L. The relationship between land surface temperature and NDVI with remote sensing: application to Shanghai Landsat 7 ETM+ data. Int J Remote Sensing. 2007;28(15):3205–26. https://doi.org/10.1080/01431160500306906.
Zhang X, Zhong T, Feng X, Wang K. Estimation of the relationship between vegetation patches and urban land surface temperature with remote sensing. Int J Remote Sensing. 2009;30(8):2105–18. https://doi.org/10.1080/01431160802549252.
Zhang Y, Odeh IO, Ramadan E. Assessment of land surface temperature in relation to landscape metrics and fractional vegetation cover in an urban/peri-urban region using Landsat data. Int J Remote Sensing. 2013;34(1):168–89. https://doi.org/10.1080/01431161.2012.712227.
Zheng B, Myint SW, Fan C. Spatial configuration of anthropogenic land cover impacts on urban warming. Landscape Urban Planning. 2014;130:104–11. https://doi.org/10.1016/j.landurbplan.2014.07.001.
Zhibin R, Haifeng Z, Xingyuan H, Dan Z, Xingyang Y. Estimation of the relationship between urban vegetation configuration and land surface temperature with remote sensing. J Indian Soc Remote Sensing. 2015;43(1):89–100. https://doi.org/10.1007/s12524-014-0373-9.
Zhou W, Huang G, Cadenasso ML. Does spatial configuration matter? Understanding the effects of land cover pattern on land surface temperature in urban landscapes. Landscape Urban Planning. 2011;102(1):54–63. https://doi.org/10.1016/j.landurbplan.2011.03.009.
Zhou W, Wang J, Cadenasso ML. Effects of the spatial configuration of trees on urban heat mitigation: A comparative study. Remote Sens Environ. 2017;195:1–12. https://doi.org/10.1016/j.rse.2017.03.043.

Publisher's Note